Dwarf males function as males but retain female-biased transcriptional profiles in an androdioecious barnacle

Kenji Toyota[a,b,c*], Asami Kajimoto[a,b], Rie Kusunoki[d], Yoichi Yusa[d]

[a]Department of Bioresource Science, Graduate School of Integrated Sciences for Life, Hiroshima University, 1-4-4, Kagamiyama, Higashihiroshima-shi, Hiroshima 739-8528, Japan.
[b]Department of Biological Sciences, Faculty of Science, Kanagawa University, 3-27-1, Rokkakubashi, Kanagawa-ku, Yokohama-city, Kanagawa, 221-8686, Japan.
[c]Department of Biological Science and Technology, Faculty of Advanced Engineering, Tokyo University of Science, 6-3-1 Niijuku, Katsushika-ku, Tokyo 125-8585, Japan.
[d]Nara Women's University, Kitauoya-nishi, 630-8506 Nara, Japan.

*Corresponding author
Email addresses: toyotak@hiroshima-u.ac.jp

Abstract

Sexual systems exhibit remarkable diversity, yet how alternative reproductive strategies are implemented at the level of gene expression remains poorly understood. In androdioecious species, males coexist with hermaphrodites and function exclusively as sperm donors, raising the question of whether the males' transcriptional profiles are fully masculinized or retain features of hermaphroditic ancestry. We investigated this question in the epizoic barnacle *Octolasmis unguisiformis* by comparing transcriptomes of male and female reproductive tissues within hermaphrodites and conspecific males that arrest growth at a young stage (dwarf males). Principal component analysis and correlation structure revealed that dwarf males cluster more closely with female tissue than with male tissue of hermaphrodites. Distributional analyses of $\log_2$ fold changes showed minimal genome-wide divergence between dwarf males and female tissue. Multivariate distance comparisons and effect size analyses further supported that transcriptomic divergence was smallest in the dwarf male–female cpmparison. In contrast, male reproductive tissue of hermaphrodites exhibited strong enrichment of genes associated with flagellated sperm motility, ciliary structure and dynein complexes. These results indicate that specialization of hermaphroditic male tissue in this species is concentrated within a discrete sperm motility module, while dwarf males retain broadly female-biased transcriptional profiles at the genome-wide scale. Our findings demonstrate that functional male identity of dwarf males can arise without wholesale transcriptional masculinization and suggest that alternative male strategies in androdioecious systems may evolve through modular activation of male-specific gene sets within a shared transcriptional background.

Keywords

Androdioecy, sex allocation, alternative reproductive strategies, gene expression divergence, sexual system evolution

1. Introduction

Sexual systems are evolutionarily labile and exhibit striking diversity across the animal kingdom, ranging from strict gonochorism to simultaneous hermaphroditism and mixed systems such as androdioecy (coexistence of males and hermaphrodites). Within such systems, and more broadly across sexually reproducing taxa, alternative male morphs frequently arise, producing discrete morphs that differ in morphology, behaviour and life-history tactics (Gross 1996; Taborsky 1998). While the ecological and selective drivers of alternative strategies are well documented, considerably less is understood about how these strategies are implemented at the level of gene expression. In particular, it remains unclear whether alternative male phenotypes are underpinned by extensive reprogramming of sex-biased transcription or instead emerge through modification of pre-existing transcriptional states (Ellegren & Parsch 2007; Mank 2017). Androdioecy, in which males coexist with hermaphrodites, represents a rare but evolutionarily important sexual system (Charnov and Bull 1977; Pannell 2002; Weeks et al. 2006). Because hermaphrodites retain both male and female reproductive functions, androdioecy offers a unique opportunity to examine how male function is partitioned and specialized across alternative morphs. In many marine invertebrates, androdioecy takes the form of coexistence of hermaphrodites and dwarf males—small individuals that attach to hermaphrodites and function exclusively as sperm donors (Ghiselin 1974; Weeks et al. 2006). These dwarf males often exhibit extreme morphological reduction relative to hermaphrodites, yet maintain full male reproductive capability. As many androdioecious species are considered to have evolved from hermaphroditic ancesters (*e.g.*, in barnacles; Yusa et al. 2013), androdioecy in these animals raises a fundamental question: does male function in dwarf males correspond to a fully masculinized transcriptional profile, or does it operate within a broader transcriptional context shaped by hermaphroditic ancestry?

Sex-biased gene expression is a primary mechanism underlying sexual differentiation and the evolution of sexual dimorphism (Ellegren & Parsch 2007; Ingleby et al. 2015). In gonochoristic species, reproductive tissues of males and females typically display extensive transcriptomic divergence, reflecting the coordinated activation of sex-specific gene networks (Mank 2017). However, in organisms where reproductive roles are subdivided within individuals or across closely related morphs, the architecture of sex-biased expression may be constrained. The extent to which alternative male phenotypes exhibit complete transcriptional masculinization, partial overlap with female-biased expression, or retention of ancestral gene expression programs remains largely unexplored. Addressing this gap is essential for understanding how sexual system evolution shapes gene regulatory architectures.

The epizoic barnacle *Octolasmis unguisiformis* provides an ideal model to investigate these questions. This species exhibits functional androdioecy: large hermaphrodites possess both male and female reproductive tissues, whereas dwarf males attach to conspecifics and function

solely as sperm donors (Sawada et al. 2015; Wijayanti et al. 2024). Developmentally, dwarf males may arise within the same genetic background as hermaphrodites, yet they are morphologically simplified and lack female reproductive structures (Sawada et al. 2015). Although their behavioural and functional roles as males are well established, the molecular basis of their sexual identity has not been examined. Specifically, it is unknown whether dwarf males exhibit transcriptional profiles comparable to male reproductive tissue within hermaphrodites, or whether they retain elements of female-biased gene expression associated with their hermaphroditic lineage. Here, we used RNA sequencing to compare gene expression among male reproductive tissue of hermaphrodites, female reproductive tissue of hermaphrodites, and conspecific dwarf males in *O. unguisiformis*. By integrating paired sampling within hermaphroditic individuals and cross-morph transcriptomic comparisons, we tested whether dwarf males exhibit male-typical transcriptional programs or instead retain female-biased transcriptional profiles. We show that although dwarf males function reproductively as males, their global transcriptomic architecture more closely resembles female tissue than male tissue within hermaphrodites. These findings provide new insight into how alternative male strategies are implemented at the level of gene expression and highlight the importance of transcriptional context in the evolution of complex sexual systems.

2. Materials and methods

2.1 Animal ethics statement

All experimental procedures were conducted in accordance with the guidelines of the Institutional Animal Care and Use Committee of Nara Women's University. Animal handling and experimental design complied with the ARRIVE guidelines for reporting animal research (Percie du Sert et al. 2020).

2.2 Sample collection and experimental design

Individuals of the host crab *Macrophthalmus milloti* carrying the androdioecious barnacle *Octolasmis unguisiformis* were collected by hand during low tides from a mud flat at Kise Bay, Amami-Oshima Island, Kagoshima Prefecture, Japan (28.424°N, 129.651°E) on 15 November 2024. After collection, host crabs were transported to the laboratory and maintained in aerated seawater under ambient temperature and salinity conditions until dissection. The experimental design consisted of four RNA-seq sample categories: male reproductive tissue of hermaphrodites (capitulum consists of prosoma and inner mantle surface, excluding shells and brooded eggs, hM), female reproductive tissue of hermaphrodites (peduncle, hF), conspecific-attached dwarf males (dM), and host crab eggs (*M. milloti* eggs) (Fig. 1). Detailed sample information, including biological replication and tissue composition, is summarized in **Table S1**. For hermaphroditic

individuals, hM and hF samples were prepared from the same individuals, enabling paired comparisons between male and female reproductive tissues within hermaphrodites. Each hermaphroditic individual constituted one biological replicate (n = 1), and samples were obtained from three individuals in total (hM, n = 3; hF, n = 3). Dwarf males were sampled as pooled biological replicates because of their extremely small body size. For each dwarf male sample, the whole boy of three individuals were pooled to form a single biological replicate (n = 1). Two independent pooled samples were prepared (dM, n = 2), each derived from a different set of individuals. One additional RNA-seq sample consisting of eggs from *M. milloti* (n = 1) was prepared exclusively for the purpose of identifying and excluding host-derived transcripts from downstream analyses. This egg sample was not included in differential expression analyses.

2.3 Dissection and RNA extraction

Barnacles were carefully detached from host crabs using fine forceps under a stereomicroscope. In hermaphroditic individuals, the peduncle was dissected as hF, whereas the capitulum was dissected as hM after removal of shells and brooded eggs. Dwarf males were processed as whole individuals including the capitulum and shell. All dissected tissues were immediately flash-frozen and stored at −80 °C. RNA extraction was performed within two months of storage. Total RNA was extracted using ISOGEN II (Nippon Gene) followed by purification with the RNeasy Micro Kit (Qiagen) according to the manufacturer's instructions. RNA concentration and purity were assessed using NanoDrop spectrophotometry (A260/280 ratio). RNA concentrations ranged from 45.2–402.6 ng/µl **(Table S1)**.

2.4 Library preparation, sequencing, and transcriptome assembly

cDNA libraries were constructed using the SureSelect Strand-Specific RNA Library Preparation Kit (Agilent Technologies, Santa Clara, CA, USA), with unique barcodes assigned to each sample. Libraries were sequenced on an Illumina NovaSeq 6000 platform using a 150 bp paired-end configuration. Raw reads have been deposited in DDBJ under accession number DRR908949-DRR908957. Raw sequencing quality was assessed using FastQC v0.11.2 (https://www.bioinformatics.babraham.ac.uk/projects/fastqc). Reads from all *O. unguisiformis* samples (hM, hF, and dM) and the host egg sample were independently assembled using Trinity v2.9.1 with default parameters in paired-end mode. Then, all downstream analyses—including redundancy reduction, transcript clustering, and expression quantification—were conducted following the same bioinformatic pipeline described in our previous study (Toyota et al. 2023). Read quantification was performed using Salmon v1.1.0 with quasi-mapping mode. Transcript clustering was conducted using Corset v1.09 to generate gene-level count matrices. To minimize potential host contamination, any cluster in which reads were detected in the egg sample of the host crab *M. milloti*

was excluded from further analyses, as such transcripts were considered likely to originate from host-derived RNA. After removal of these clusters, additional filtering was applied to exclude lowly expressed clusters with fewer than 50 total reads across all samples prior to differential expression analysis. Transcriptome completeness was evaluated using BUSCO (eukaryote_odb10 dataset). Subsequent analyses were conducted using filtered transcript sets from hM (n = 3), hF (n = 3), and dM (n = 2). The egg sample was not included in downstream expression analyses.

2.5 Differential expression and multivariate analyses

Differentially expressed transcripts (DETs; false discovery rate, FDR < 0.05) were identified using DESeq2 implemented in the SARTools package v1.6.6 (Varet et al. 2016), based on count data generated by Corset. Pairwise comparisons were conducted between hM and hF (paired design), hM and dM, and hF and dM. Principal component analysis (PCA) was performed using SARTools to assess global expression patterns across all samples and to visualize relationships among reproductive contexts. Pairwise transcriptomic distances were calculated using Euclidean distance based on vst-transformed expression values. Differences among groups were tested using PERMANOVA implemented in the vegan package (adonis2 function) with 999 permutations.

2.6 Functional annotation and enrichment analyses

Functional annotation was performed using BLASTX against the NCBI non-redundant protein database and the *Drosophila melanogaster* protein dataset (Drosophila_melanogaster.BDGP6.46.pep.all.fa) with AC-DIAMOND (E-value threshold = 1e−3). Gene Ontology (GO) and Kyoto Encyclopedia of Genes and Genomes (KEGG) enrichment analyses were conducted using the DAVID database (Dennis et al. 2003; last accessed 9 February 2026) based on biased DET sets. Only enrichment results that remained significant after multiple-testing correction were considered.

3. Results

3.1 Sampling design and transcriptome completeness

A total of eight transcriptome libraries were analysed, comprising three paired hermaphroditic individuals from which male (hM; n = 3) and female (hF; n = 3) tissues were dissected, and two pools of conspecific-attached dwarf males (dM; n = 2; **Fig. 1**; **Table S1**). The paired design enabled direct within-individual comparisons of male and female reproductive functions in hermaphrodites. BUSCO analysis indicated high transcriptome completeness **(Table S2),** with 255 of 255 eukaryote BUSCO groups recovered as complete (100%), and no fragmented or missing BUSCOs. The majority of complete BUSCOs were duplicated (82.7%), consistent with clustering at the Corset-

defined gene level. These results confirm that the reference assembly provided a robust basis for downstream expression analyses.

3.2 Global transcriptomic structure across reproductive contexts

PCA based on gene-wise scaled $\log_2$-transformed expression values separated samples primarily along PC1 (31.4% of variance; **Fig. 2A**). Female reproductive tissues of hermaphrodites (hF) clustered distinctly from male reproductive tissues (hM). Dwarf males (dM) positioned closer to hF than to hM along PC1, indicating greater global transcriptional similarity to female tissue. Importantly, black lines connecting hM and hF samples from the same individual demonstrate consistent within-individual divergence between male and female tissues **(Fig. 2A)**, validating the paired design. Pearson correlation analysis further revealed that expression profiles among hF samples were highly correlated, and that dM samples showed stronger similarity to hF than to hM **(Fig. 2B)**. Distributional analysis of mean TPM-based $\log_2$ fold changes showed that the dM–hF contrast exhibited the strongest concentration of values near zero **(Fig. 2C)**, indicating minimal genome-wide transcriptional divergence between dwarf males and female tissue. In contrast, both hM–hF and hM–dM distributions were broader, reflecting greater transcriptomic differentiation involving hM **(Fig. 2C)**. Thus, at the global level, dwarf males are transcriptionally closer to female tissue than to male tissue within hermaphrodites.

Euclidean distances calculated in multivariate expression space further quantified transcriptomic divergence among reproductive contexts **(Fig. 2D)**. The smallest inter-group distances were observed between dM and hF, whereas distances involving hM were consistently larger. PERMANOVA detected significant overall differentiation among groups ($R^2 = 0.980$, $p = 0.025$; **Fig. 2D**). However, effect size analyses provided additional insight into the magnitude and direction of divergence. Cliff's δ estimates with 95% bootstrap confidence intervals demonstrated that the contrast between hM and hF showed the largest effect size, followed by hM–dM, whereas dM–hF exhibited the smallest effect size and confidence intervals overlapping zero **(Fig. S1).** MA plots for all three pairwise contrasts further illustrate that expression differences are broadly distributed in hM–hF and hM–dM comparisons **(Fig. S2A–C)**, whereas the dM–hF contrast shows markedly fewer transcripts with large $\log_2$ fold changes. Together, these analyses confirm that dwarf males are transcriptomically most similar to female reproductive tissue rather than to hermaphroditic male tissue.

3.3 Differential expression between male and female tissues within hermaphrodites

Comparison between male (hM) and female (hF) reproductive tissues of hermaphrodites identified 2,514 differentially expressed transcripts (DETs) at FDR < 0.05 **(Table S3)**. Among these, 2,088 transcripts were upregulated in hM, whereas 426 transcripts were upregulated in hF, indicating

pronounced transcriptional asymmetry between male and female reproductive functions within hermaphroditic individuals. hM-enriched transcripts included numerous sperm-associated genes, including spermatogenesis-associated protein 17-like, sperm flagellar protein 1-like, motile sperm domain-containing protein 2-like, and cation channel sperm-associated proteins **(Table 1)**. In contrast, hF-enriched transcripts were dominated by vitellogenin-1-like and vitellogenin receptor genes **(Table 1)**. GO enrichment analysis identified significant overrepresentation of sperm motility–related categories in hM, including flagellated sperm motility, cilium movement, and dynein complex **(Table 2)**.

GO enrichment in hF highlighted transcription-related categories, including: regulation of DNA-templated transcription, RNA polymerase II-specific DNA-binding transcription factor activity, zinc ion binding, and nuclear receptor activity **(Table 2)**. Thus, male–female differentiation within hermaphrodites is characterized by strong, functionally coherent gene expression divergence.

3.4 Transcriptomic contrasts involving dwarf males

Comparison between hM and dM identified 2,548 differentially expressed transcripts (DETs) at FDR < 0.05 **(Table S4)**, comprising 1,807 transcripts upregulated in hM and 741 upregulated in dM. Despite both representing male reproductive contexts, this large number of DETs indicates substantial transcriptional differentiation. Functional enrichment analyses revealed that transcripts upregulated in hM were strongly enriched for sperm motility–related categories, including: flagellated sperm motility, cilium movement involved in cell motility, dynein complex, and Motor proteins **(Table 2; Table S7)**. These enrichments reflect elevated activation of the sperm motility module in hermaphroditic male tissue. MA plots illustrate broad distribution of large $\log_2$ fold changes across transcripts **(Fig. S2B)**, confirming extensive divergence between hM and dM. Although dwarf males function reproductively as males, they do not match the transcriptional intensity of sperm-associated pathways observed in hermaphroditic male tissue.

In contrast, comparison between dM and hF yielded only 116 DETs **(Table S5)**, comprising 14 transcripts upregulated in dM and 102 transcripts upregulated in hF. This number is more than twenty-fold lower than the number of DETs identified in contrasts involving hM. The distribution of $\log_2$ fold changes in the dM–hF comparison is strongly centered around zero **(Fig. 2C)**, and MA plots show markedly fewer transcripts with large absolute fold changes **(Fig. S2C)**. Multivariate analyses further support this pattern. PCA positions dwarf males closer to hF than to hM **(Fig. 2A)**, correlation clustering groups dM with hF **(Fig. 2B)**, and Euclidean distances are smallest for the dM–hF comparison **(Fig. 2D)**. Cliff's δ effect size estimates confirm that transcriptomic divergence between dM and hF is minimal, with confidence intervals overlapping zero **(Fig. S1)**.

Together, these results reveal a striking asymmetry in transcriptional divergence involving dwarf males: extensive divergence between hM and dM (2,548 DETs), extensive divergence between hM and hF (2,514 DETs), and minimal divergence between dM and hF (116 DETs). Thus, dwarf males are transcriptionally far closer to female reproductive tissue than to hermaphroditic male tissue at the genome-wide scale. Although dwarf males express a subset of male-associated genes sufficient for reproductive function, their overall transcriptomic state remains predominantly female-like.

Discussion

4.1 Dwarf males retain female-biased transcription despite functional male identity

Our transcriptomic analyses demonstrate that dwarf males of *O. unguisiformis* cluster more closely with female reproductive tissue of hermaphrodites than with male reproductive tissue. Despite functioning exclusively as sperm donors, dwarf males do not exhibit a fully masculinized transcriptional architecture. Instead, they retain a substantial component of female-biased gene expression at the genome-wide scale. This pattern is consistently supported across analytical approaches. PCA **(Fig. 2A)**, correlation structure **(Fig. 2B)**, fold-change distributions **(Fig. 2C)**, and multivariate distances **(Fig. 2D)** all indicate greater similarity between dwarf males and female tissue than between dwarf males and hermaphrodite male tissue. Importantly, effect size estimates based on Cliff's δ demonstrate that transcriptomic divergence between dwarf males and female tissue is markedly smaller than that between hermaphroditic male and female tissues **(Fig. S1)**. Consistent with this pattern, MA plots show reduced numbers and magnitudes of differentially expressed transcripts in the dM–hF contrast relative to contrasts involving hM **(Fig. S2A–C)**. Thus, female-like similarity of dwarf males is not merely a qualitative observation but quantitatively robust across metrics. In gonochoristic species, male and female reproductive tissues typically show extensive divergence driven by sex-biased gene expression (Ellegren & Parsch 2007; Mank 2017). Our results contrast with this canonical pattern: in *O. unguisiformis*, male function does not correspond to wholesale transcriptional masculinization.

One potential concern is whether the observed transcriptomic similarity between dM and hF reflects genuine sex-biased expression rather than a tissue-type confound arising from the different body regions sampled. In this study, hM samples derive from the capitulum of hermaphrodites, hF samples from the peduncle, and dM samples from whole individuals including the capitula and the peduncles. If tissue identity alone drove the patterns, dM samples—which include capitulum tissue—would be expected to resemble hM (also capitulum-derived) rather than hF (peduncle-derived). The opposite result was observed consistently across all multivariate analyses: dM clustered with hF and showed smaller Euclidean distances to hF than to hM.

Furthermore, the genes most strongly differentiating hM from both hF and dM encode sperm-specific functional proteins (e.g., sperm flagellar proteins, cation channel sperm-associated proteins), whose tissue-specific expression is unlikely to be explained by anatomical region alone. Taken together, these observations argue against a simple tissue-type artifact and instead support the interpretation that the female-like transcriptional state of dwarf males reflects a genuine aspect of their reproductive biology.

4.2 Male specialization is concentrated within a sperm motility module

Although global transcriptomic divergence between dwarf males and female tissue was limited, male reproductive tissue of hermaphrodites exhibited strong enrichment of genes associated with flagellated sperm motility, ciliary structure, dynein complexes and microtubule-based transport. These gene categories represent conserved components of metazoan sperm motility machinery. Notably, barnacles are unique among crustaceans in possessing motile sperm, a trait linked to internal fertilization within the enclosed mantle cavity (Høeg et al. 2015). This phylogenetically distinctive feature may explain why the sperm motility module is particularly pronounced in barnacle male tissue. The enrichment of these functions in hermaphroditic male tissue indicates that male specialization is concentrated within a discrete functional module. In contrast, dwarf males displayed reduced expression of this sperm-associated module relative to hermaphroditic male tissue, despite maintaining male reproductive capability. This suggests that the alternative male strategy in this species is achieved through quantitative modulation of a specific gene set rather than genome-wide transcriptional reprogramming. Such modular organization of sex-biased gene expression is consistent with studies showing that a relatively small subset of genes often drives major sexual divergence (Ingleby et al. 2015). In *O. unguisiformis*, male function appears to depend primarily on activation of this sperm motility module superimposed upon a largely shared transcriptional background.

4.3 Alternative male strategies without extensive transcriptional rewiring

Alternative reproductive strategies frequently involve dramatic morphological and behavioural divergence (Gross 1996; Taborsky 1998). However, the degree to which such strategies require extensive transcriptional differentiation remains unclear. Our results indicate that in an androdioecious barnacle, the alternative male strategy represented by dwarf males does not require large-scale rewiring of gene expression networks. Instead, dwarf males retain female-biased transcriptional features while selectively expressing genes necessary for sperm production. This pattern suggests that alternative male strategies can emerge through localized activation of male-specific modules rather than through the evolution of an entirely distinct male transcriptome. In systems where hermaphrodites retain both reproductive functions, the regulatory landscape

underlying female-biased genes may remain active even in morphs specialized for male function.

4.4 Contrasting patterns in androdioecious nematodes

The molecular implementation of androdioecy differs strikingly among taxa. In nematodes such as *Caenorhabditis elegans*, transcriptomic comparisons between males and hermaphrodites reveal extensive male-specific gene expression. Ebbing et al. (2018) demonstrated that most sperm-related genes are expressed specifically in males and that male sperm outcompete those produced by hermaphrodites. Haque et al. (2024) further showed that male-biased genes are preferentially lost in hermaphroditic lineages, suggesting substantial genomic restructuring following the evolution of hermaphroditism. Although these studies did not separate male and female tissues within hermaphroditic individuals, they consistently identified clearly masculinized transcriptional states in males. This contrasts with our findings in *O. unguisiformis*, where dwarf males do not exhibit comparably distinct male transcriptomes. These differences may reflect contrasting evolutionary origins. Androdioecious nematodes are considered to have evolved from dioecious ancestors (Guo et al. 2009; Kiontke et al. 2011; Thomas et al. 2012), and subsequent gene loss likely contributed to derived genomic architectures (Rödelsperger et al. 2018). In such systems, the transition to hermaphroditism involved substantial reconfiguration of male-biased gene content. In contrast, *O. unguisiformis* hermaphrodites simultaneously retain male and female functions, and dwarf males likely evolved within this hermaphroditic framework (Yusa et al., 2013). As a result, the emergence of dwarf males may not have required genome-wide remodeling of sex-biased transcription.

4.5 Evolutionary implications for sexual system diversification

Our findings suggest that the evolution of alternative male strategies in androdioecious systems can proceed without complete transcriptional masculinization. In *O. unguisiformis*, male reproductive function is concentrated within a specialized sperm motility module, whereas the broader transcriptional landscape remains largely shared with female tissue. The consistency of this pattern across PCA, fold-change distributions, multivariate distances and non-parametric effect size estimates **(Fig. 2; Fig. S1)** indicates that dwarf males occupy a transcriptional state that is quantitatively closer to female tissue than to hermaphroditic male tissue. This convergence across analytical frameworks strengthens the inference that dwarf males retain female-biased transcription at the genome-wide scale. Such partial decoupling between functional male identity and global transcriptional state highlights how sexual systems may evolve through modular activation of male-specific gene sets within a shared regulatory background. In fact, in a congener *O. warwickii*, dwarf males retain the ability to become hermaphroditic, and a small proportion of them realize this (Wijayanti and Yusa, 2016). This interspecific comparison and the results of this study in common suggest that dwarf males in *Octolasmis* spp. are virtually hermaphrodites that arrest growth and

allocate most of the resources to the male function. The degree of transcriptional differentiation between reproductive morphs may therefore depend not only on current sexual roles but also on historical and developmental constraints shaping the underlying gene regulatory architecture.

5. Conclusions

By combining paired sampling within hermaphrodites and comparative transcriptomics across reproductive morphs, we show that dwarf males in *O. unguisiformis* function reproductively as males while retaining female-biased transcriptional profiles. Male specialization is concentrated within a discrete sperm motility module rather than across the genome. These findings provide new insight into how alternative male strategies are implemented at the molecular level and demonstrate that sexual function and global transcriptional identity can become partially decoupled during the evolution of complex sexual systems.

Author Contributions

K.T. and Y.Y. designed the research. K.T. and A.K. conducted data analyses and wrote the original draft of the manuscript. R.M. provided materials. All authors reviewed the manuscript and approved the final submission.

Acknowledgements

The computation was performed using Research Center for Computational Science, Okazaki, Japan (Project: NIBB, 25-IMS-C236).

Funding

This work was supported by JSPS KAKENHI Grant Number 24K02100 to Y.Y. and NIBB Collaborative research projects for Trans-Scale Biology (25NIBB103) to K.T.

Disclosure

Benefit-Sharing Statement: Benefits from this research accrue from sharing our data and results deposited in DDBJ (accession DRR908949-DRR908957).

Conflicts of Interest

The authors declare no conflicts of interest.

Data Availability Statement

Data supporting conclusions of this study have been deposited in DDBJ (accession DRR908949-

DRR908957).

References

Charnov, E. L., and J. Bull. 1977. “When is sex environmentally determined?” *Nature* 266: 828–830. https://doi.org/10.1038/266828a0

Dennis, G. Jr., Sherman, B. T., Hosack, D. A., Yang, J., Gao, W., Lane, H. C., and R. A. Lempicki. 2003. “DAVID: Database for annotation, visualization, and integrated discovery.” *Genome Biology* 4: P3. https://doi.org/10.1186/gb-2003-4-5-p3

Ebbing, A., Vértesy, Á., Betist, M. C., Spanjaard, B., Junker, J.P., Berezikov, E., Van Oudenaarden, A. and Korswagen, H.C. 2018. Spatial transcriptomics of *C. elegans* males and hermaphrodites identifies sex-specific differences in gene expression patterns. *Developmental Cell 47*: 801–813. https://doi.org/10.1016/j.devcel.2018.10.016

Ellegren, H., and J. Parsch. 2007. “The evolution of sex-biased genes and sex-biased gene expression.” *Nature Reviews Genetics* 8: 689–698. https://doi.org/10.1038/nrg2167

Ghiselin M. T. 1974. The economy of nature and the evolution of sex. University of California Press.

Guo Y, Lang S, Ellis RE. 2009. Independent recruitment of F box genes to regulate hermaphrodite development during nematode evolution. Current Biology. 19:1853–1860. 10.1016/j.cub.2009.09.042

Gross, M R. 1996. “Alternative reproductive strategies and tactics: diversity within sexes.” *Trends in Ecology & Evolution* 11: 92–98. https://doi.org/10.1016/0169-5347(96)81050-0

Haque, R., Kurien, S.P., Setty, H., Salzberg, Y., Stelzer, G., Litvak, E., Gingold, H., Rechavi, O. and M. Oren-Suissa. 2024. “Sex-specific developmental gene expression atlas unveils dimorphic gene networks in *C. elegans*.” *Nature Communications* 15: 4273. https://doi.org/10.1038/s41467-024-48369-z

Høeg, J. T., Yusa, Y., and N. Dreyer. 2015. “Sex determination in the androdioecious barnacle *Scalpellum scalpellum* (Crustacea: Cirripedia).” *Biological Journal of the Linnean Society* 54: 181–198. https://doi.org/10.1111/bij.12735

Ingleby, F. C., Flis, I., and E. H. Morrow 2015. “Sex-biased gene expression and sexual conflict throughout development.” *Cold Spring Harbor Perspectives in Biology* 7: a017632. https://doi.org/10.1101/cshperspect.a017632

Kiontke K. C., Félix M. A., Ailion M., Rockman M. V., Braendle C., Pénigault J. B., Fitch D. H. A. 2011. A phylogeny and molecular barcodes for *Caenorhabditis*, with numerous new species from rotting fruits. *BMC Evolutionary Biology* 11: 339. doi: 10.1186/1471-2148-11-339.

Mank, J. E. 2017. “The transcriptional architecture of phenotypic dimorphism.” *Nature Ecology & Evolution* 1: 6. https://doi.org/10.1038/s41559-016-0006

Pannell, J. R. 2002. “The Evolution and Maintenance of Androdioecy.” *Annual Review of Ecology, Evolution, and Systematics* 33: 397–425. https://doi.org/10.1146/annurev.ecolsys.33.010802.150419

Percie, du Sert N., Hurst, V., Ahluwalia, A., Alam, S., Avey, M. T., Baker, M., Browne, W. J., Clark, A., Cuthill, I. C, Dirnagl, U., Emerson, M., et al., 2020. “The ARRIVE guidelines 2.0: updated guidelines for reporting animal research.” *PLoS Biology* 18: e3000410. https://doi.org/10.1371/journal.pbio.3000410

Rödelsperger, C., Röseler, W., Prabh, N., Yoshida, K., Weiler, C., Herrmann, M. and Sommer, R.J. 2018. Phylotranscriptomics of *Pristionchus* nematodes reveals parallel gene loss in six hermaphroditic lineages. *Current Biology* 28: 3123–3127. https://doi.org/10.1016/j.cub.2018.07.041

Sawada, K., Yoshida, R., Yasuda, K., Yamaguchi, S., and Y. Yusa. 2015. “Dwarf males in the epizoic barnacle *Octolasmis unguisiformis* and their implications for sexual system evolution.” *Invertebrate Biology* 134, 162–167. https://doi.org/10.1111/ivb.12083

Taborsky, M. 1998. “Sperm competition in fish: `bourgeois' males and parasitic spawning.” *Trends in Ecology & Evolution* 13: 222–227. https://doi.org/10.1016/s0169-5347(97)01318-9

Thomas, C. G., Woodruff, G. C. and E.S. Haag. 2012. “Causes and consequences of the evolution of reproductive mode in *Caenorhabditis nematodes*.” *Trends in Genetics* 28: 213–220. https://doi.org/10.1016/j.tig.2012.02.007

Toyota, K., Yamamoto, T., Mori, T., Mekuchi, M., Miyagawa, S., Ihara, M., Shigenobu, S., and T. Ohira. 2023. “Eyestalk transcriptome and methyl farnesoate titers provide insight into the physiological changes in the male snow crab, *Chionoecetes opilio*, after its terminal molt.” *Scientific Reports* 13: 7204. https://doi.org/10.1038/s41598-023-34159-y

Varet, H., Brillet-Guéguen, L., Coppée, J. Y., and M. A. Dillies. 2016. “SARTools: A DESeq2- and EdgeR-based R pipeline for comprehensive differential analysis of RNA-seq data.” *PLoS One* 11: e0157022. https://doi.org/10.1371/journal.pone.0157022

Weeks, S. C., Benvenuto, C., and S. K. Reed. 2006. “When males and hermaphrodites coexist: a review of androdioecy in animals.” *Integrative and comparative biology* 46: 449–464. https://doi.org/10.1093/icb/icj048

Wijayanti, H., and Yusa, Y. 2016. “Plastic sexual expression in the androdioecious barnacle Octolasmis warwickii (Cirripedia: Pedunculata).” *The Biological Bulletin* 230: 51–55. https://doi.org/10.1086/BBLv230n1p51

Wijayanti, H., Sawada, K., Yasuda, K., and Y. Yusa. 2024. “Labile sex allocation and sex ratio in the androdioecious barnacle *Octolasmis unguisiformis*.” *Biological Journal of the Linnean Society* 143: blae083. https://doi.org/10.1093/biolinnean/blae083

Yusa, Y., Takemura, M., Sawada, K., and Yamaguchi, S. 2013. “Diverse, continuous, and plastic

sexual systems in barnacles." *Integrative and Comparative Biology* 53: 701–712. https://doi.org/10.1093/icb/ict016

Figure caption

Figure 1. Reproductive morphs of *Octolasmis unguisiformis*.
Crab-attached hermaphrodite (A) and conspecific-attached dwarf male (B). Both possess a penis, testis, and seminal vesicle filled with sperm; however, the hermaphrodite additionally has an ovary and egg chambers housing eggs as female reproductive structures.

Figure 2. Global transcriptomic structure across reproductive contexts.
(A) Principal component analysis (PCA) based on gene-wise scaled $\log_2$-transformed expression values for male reproductive tissue of hermaphrodites (hM; n = 3), female reproductive tissue of hermaphrodites (hF; n = 3), and dwarf males (dM; n = 2). Black lines connect paired hM and hF samples from the same hermaphroditic individual. PC1 and PC2 explain 31.4% and 16.4% of total variance, respectively. (B) Pearson correlation heatmap of variance-stabilized expression values. Samples are hierarchically clustered based on correlation distance. Dwarf males show stronger correlation with hF than with hM. (C) Distribution of mean TPM-based $\log_2$ fold changes for pairwise contrasts (hM–hF, hM–dM, dM–hF). All distributions are plotted on a common x-axis scale. The dM–hF contrast exhibits the strongest concentration around zero, indicating minimal genome-wide transcriptional divergence. (D) Euclidean transcriptomic distances among reproductive contexts calculated from variance-stabilized expression values. Boxplots represent pairwise inter-group distances. PERMANOVA indicated significant overall differentiation among groups (R^2 = 0.980, p = 0.025). Distances are smallest between dM and hF, supporting their transcriptomic similarity.

Figure S1. Cliff's δ effect sizes for pairwise transcriptomic distance contrasts
Forest plot showing Cliff's δ effect size estimates with 95% bootstrap confidence intervals for pairwise comparisons of transcriptomic distances among reproductive contexts. Positive values indicate greater divergence in the first contrast relative to the second. The hM–hF contrast shows the largest effect size, followed by hM–dM, whereas the dM–hF comparison exhibits the smallest effect size with confidence intervals overlapping zero. These results quantitatively support the conclusion that dwarf males are transcriptomically more similar to female reproductive tissue than to hermaphroditic male tissue.

Figure S2. Differential expression patterns across reproductive contexts.

MA plots for (A) hM vs hF, (B) hM vs dM, and (C) dM vs hF comparisons. Each point represents a transcript cluster. Red points indicate differentially expressed transcripts (FDR < 0.05). The dM–hF contrast shows markedly fewer transcripts with large absolute $\log_2$ fold changes, consistent with reduced transcriptomic divergence.

Fig 1

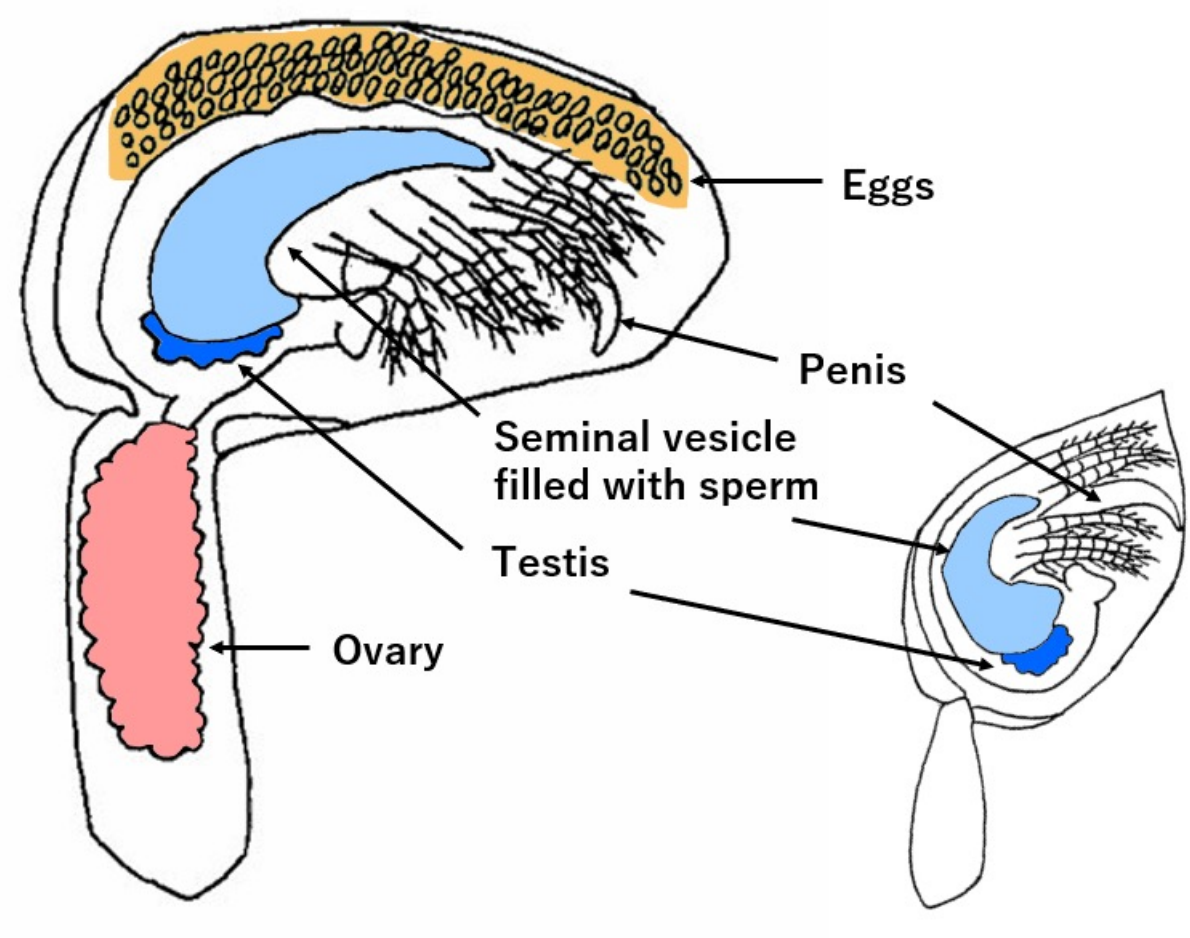

(A) Crab-attached hermaphrodite

(B) Conspecific-attached dwarf male

Fig 2

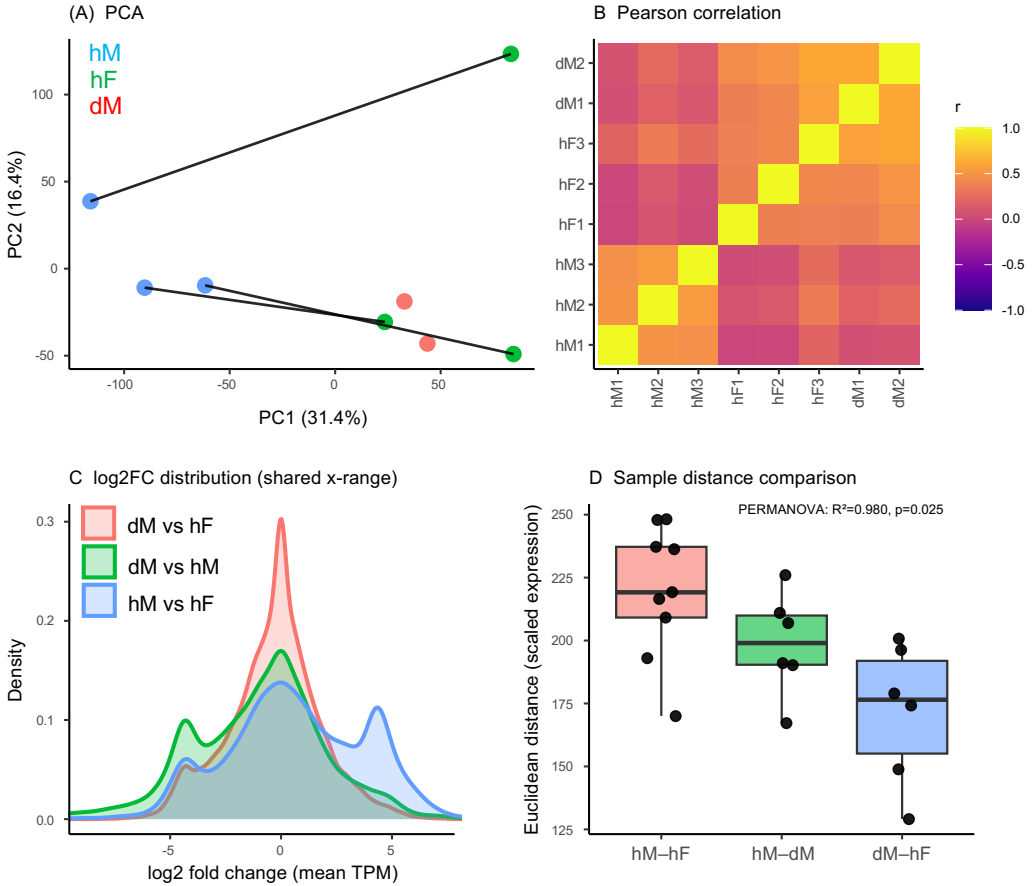
(A) PCA
hM
hF
dM
PC2 (16.4%)
PC1 (31.4%)
B Pearson correlation
dM2
dM1
hF3
hF2
hF1
hM3
hM2
hM1
r
1.0
0.5
0.0
-0.5
-1.0
C log2FC distribution (shared x-range)
dM vs hF
dM vs hM
hM vs hF
Density
log2 fold change (mean TPM)
D Sample distance comparison
PERMANOVA: R²=0.980, p=0.025
Euclidean distance (scaled expression)
hM–hF
hM–dM
dM–hF

Fig S1

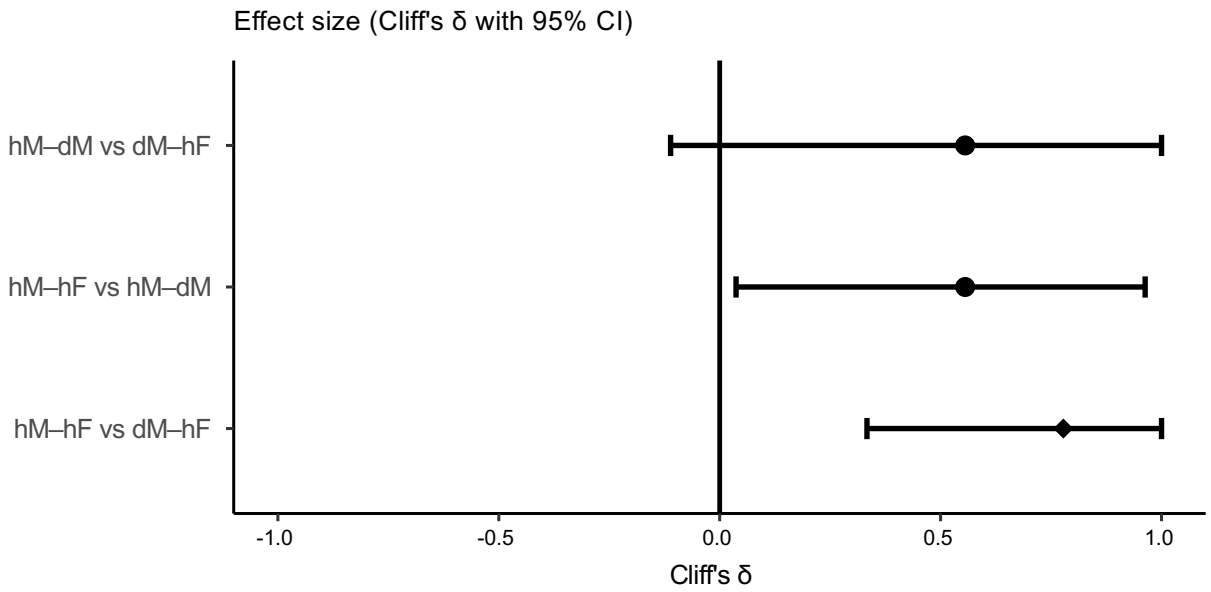
Effect size (Cliff's δ with 95% CI)
hM–dM vs dM–hF
hM–hF vs hM–dM
hM–hF vs dM–hF
-1.0
-0.5
0.0
0.5
1.0
Cliff's δ

Fig S2

(A) hF vs hM

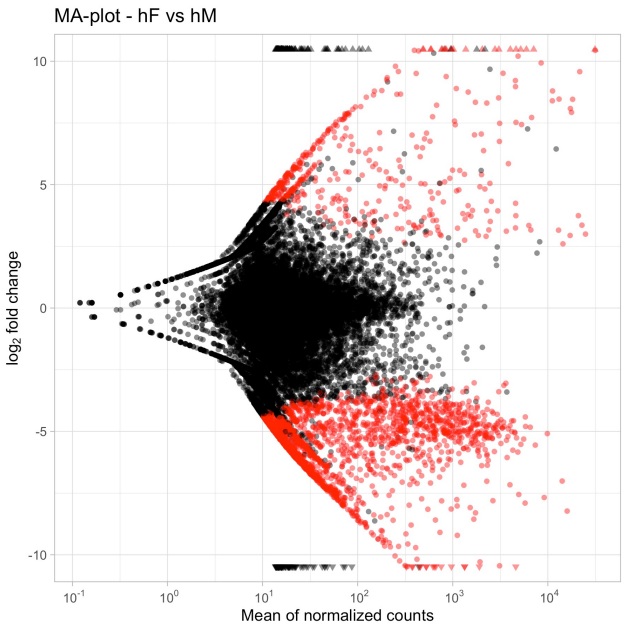

(B) dM vs hM

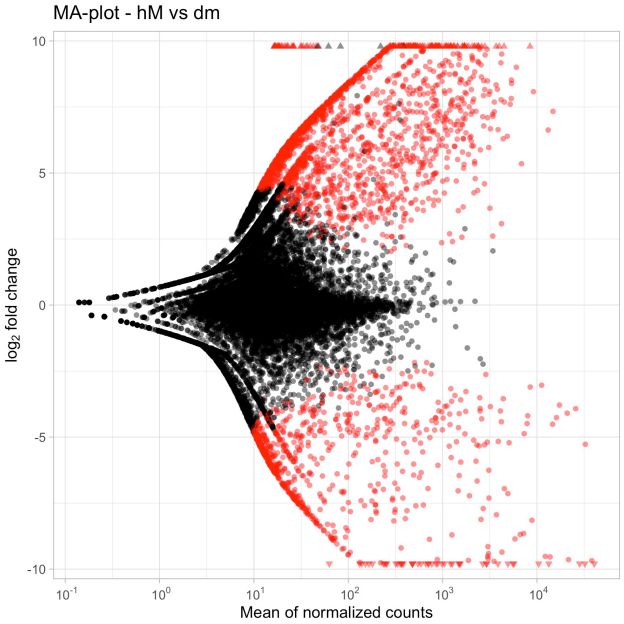

(C) dM vs hF

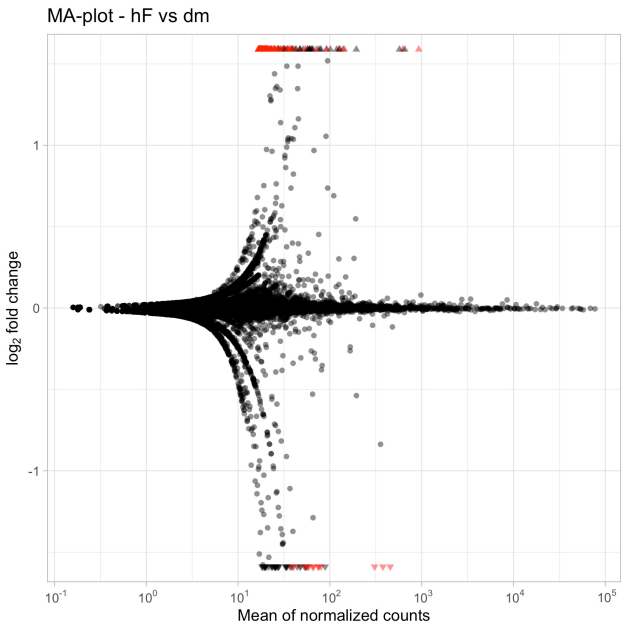

Table 1. Top hits of differential expressed transcripts.

Table 1

hM-enriched (hF vs hM)	hM1	hM2	hM3	hF1	hF2	hF3	log2FoldChange	pvalue	padj	description
Cluster-60992.0	1184	410	924	70	0	18	-3.946	0.002965656	0.023255152	spermatogenesis-associated protein 17-like [Pollicipes pollicipes]
Cluster-63311.0	2519	1531	2780	0	0	134	-4.247	0.00457293	0.030629777	motile sperm domain-containing protein 2-like [Pollicipes pollicipes]
Cluster-62067.0	258	212	246	0	3	18	-4.266	0.001173952	0.012307058	cation channel sperm-associated protein 2-like [Pollicipes pollicipes]
Cluster-61615.0	592	265	542	0	15	20	-4.518	0.000460693	0.006760384	sperm flagellar protein 1-like [Amphibalanus amphitrite]
Cluster-58367.0	44	52	0	0	0	0	-4.559	0.008148696	0.043912804	spermatogenesis-associated protein 17-like [Pollicipes pollicipes]
Cluster-62820.0	3317	1969	2461	0	0	114	-4.662	0.002105375	0.018580816	sperm surface protein Sp17 [Amphibalanus amphitrite]
Cluster-55553.1	546	449	562	3	0	19	-5.265	7.25E-05	0.001847551	cation channel sperm-associated protein 3-like [Amphibalanus amphitrite]
Cluster-26553.9034	521	316	545	0	0	10	-5.86	4.42E-05	0.001268595	sperm flagellar protein 2-like [Amphibalanus amphitrite]

hF-enriched (hF vs hM)	hM1	hM2	hM3	hF1	hF2	hF3	log2FoldChange	pvalue	padj	description
Cluster-26553.13583	0	0	0	483	243	4375	11.483	8.62E-11	2.60E-08	vitellogenin-1-like [Pollicipes pollicipes]
Cluster-26553.13631	1	5	0	2542	385	3602	8.895	1.43E-10	3.86E-08	vitellogenin-1-like [Pollicipes pollicipes]
Cluster-26553.14066	0	0	0	127	17	933	8.813	3.38E-07	3.00E-05	vitellogenin-1-like [Pollicipes pollicipes]
Cluster-26553.13580	0	0	5	701	368	2980	8.221	2.51E-08	3.41E-06	vitellogenin-1-like [Pollicipes pollicipes]
Cluster-26553.13630	0	0	0	196	9	51	6.731	6.92E-05	0.001791571	vitellogenin-1-like [Pollicipes pollicipes]
Cluster-26553.13582	0	0	0	17	29	61	5.373	0.001450038	0.01418962	vitellogenin-1-like [Pollicipes pollicipes]
Cluster-26553.11448	54	43	3	4582	4028	9851	6.752	1.13E-08	1.86E-06	putative vitellogenin receptor [Amphibalanus amphitrite]

dM-enriched (dM vs hM)	dM1	dM2	mH1	mH2	mH3	log2FoldChange	pvalue	padj	description
Cluster-26553.13583	889	1512	0	0	0	-11.659	2.18E-14	4.00E-12	vitellogenin-1-like [Pollicipes pollicipes]
Cluster-26553.13632	805	865	0	0	0	-11.183	2.13E-13	2.51E-11	vitellogenin-1-like [Pollicipes pollicipes]
Cluster-26553.13580	1216	6200	0	0	4	-10.336	1.20E-12	1.08E-10	vitellogenin-1-like [Pollicipes pollicipes]
Cluster-26553.14066	195	501	0	0	0	-9.891	5.21E-10	2.06E-08	vitellogenin-1-like [Pollicipes pollicipes]
Cluster-26553.13631	2394	1995	1	4	0	-9.636	1.99E-14	3.75E-12	vitellogenin-1-like [Pollicipes pollicipes]
Cluster-26553.13630	165	177	0	0	0	-8.892	4.57E-08	1.09E-06	vitellogenin-1-like [Pollicipes pollicipes]
Cluster-26553.13582	115	223	0	0	0	-8.851	6.94E-08	1.61E-06	vitellogenin-1-like [Pollicipes pollicipes]
Cluster-26553.13629	15	342	0	0	0	-8.59	1.70E-06	3.00E-05	vitellogenin-1-like [Pollicipes pollicipes]
Cluster-26553.13573	5	112	0	0	0	-6.714	0.000446054	0.004170214	vitellogenin-1-like [Pollicipes pollicipes]
Cluster-26553.13574	2	145	0	0	1	-6.287	0.000664642	0.005851317	vitellogenin-3-like [Amphibalanus amphitrite]
Cluster-26553.13650	38	37	0	0	0	-6.119	0.001081004	0.00865746	vitellogenin-1-like [Pollicipes pollicipes]
Cluster-26553.13572	29	43	0	0	0	-5.978	0.001418116	0.010795352	vitellogenin-1-like [Pollicipes pollicipes]
Cluster-26553.22523	55	79	0	2	0	-5.765	0.000504541	0.004616107	vitellogenin-3-like [Amphibalanus amphitrite]
Cluster-26553.14065	16	52	0	0	0	-5.702	0.002340151	0.016234245	vitellogenin-1-like [Pollicipes pollicipes]
Cluster-26553.13648	25	32	0	0	0	-5.321	0.003964698	0.024614337	vitellogenin-like [Amphibalanus amphitrite]
Cluster-26553.11448	7548	10987	40	37	2	-7.942	6.46E-12	4.68E-10	putative vitellogenin receptor [Amphibalanus amphitrite]

hM-enriched (dM vs hM)	dM1	dM2	mH1	mH2	mH3	log2FoldChange	pvalue	padj	description
Cluster-62067.0	5	17	188	184	195	3.878	0.000225692	0.002288497	cation channel sperm-associated protein 2-like [Pollicipes pollicipes]
Cluster-26553.9034	5	1	379	274	433	6.422	1.23E-08	3.32E-07	sperm flagellar protein 2-like [Amphibalanus amphitrite]
Cluster-63311.0	19	12	1835	1327	2208	6.613	1.03E-12	9.53E-11	motile sperm domain-containing protein 2-like [Pollicipes pollicipes]
Cluster-61615.0	5	0	431	229	431	6.615	1.30E-07	2.89E-06	sperm flagellar protein 1-like [Amphibalanus amphitrite]
Cluster-62820.0	28	3	2416	1706	1954	6.622	1.92E-09	6.38E-08	Sperm surface protein Sp17 [Amphibalanus amphitrite]
Cluster-63817.1	0	4	174	434	417	6.916	1.85E-07	4.00E-06	cation channel sperm-associated protein subunit gamma [Amphibalanus amphitrite]
Cluster-60992.0	5	0	862	356	734	7.409	2.95E-09	9.48E-08	spermatogenesis-associated protein 17-like [Pollicipes pollicipes]
Cluster-42605.1	0	0	231	122	151	8.414	2.85E-07	5.90E-06	cation channel sperm-associated protein 1-like [Pollicipes pollicipes]
Cluster-55553.1	0	0	398	389	446	9.675	1.26E-09	4.42E-08	cation channel sperm-associated protein 3-like [Amphibalanus amphitrite]

Table 2. Top hits of gene ontology term

Category	Term	Genes	Count	List Total	Pop Hits	Pop Total	P-Value	FDR
hF-enriched (hF vs hM)								
GOTERM_BP_DIRECT	regulation of DNA-templated transcription	0.2	10	46	506	12796	5.47E-05	1.35E-02
GOTERM_BP_DIRECT	regulation of transcription by RNA polymerase II	0.2	10	46	624	12796	2.69E-04	3.31E-02
GOTERM_MF_DIRECT	RNA polymerase II cis-regulatory region sequence-specific DNA binding	0.2	10	46	362	12822	3.72E-06	3.42E-04
GOTERM_MF_DIRECT	sequence-specific DNA binding	0.2	8	46	217	12822	9.49E-06	3.52E-04
GOTERM_MF_DIRECT	DNA-binding transcription factor activity, RNA polymerase II-specific	0.2	10	46	416	12822	1.15E-05	3.52E-04
GOTERM_MF_DIRECT	DNA-binding transcription factor activity	0.2	8	46	283	12822	5.24E-05	1.21E-03
GOTERM_MF_DIRECT	zinc ion binding	0.2	11	46	978	12822	1.74E-03	3.19E-02
GOTERM_MF_DIRECT	nuclear receptor activity	0.1	3	46	23	12822	2.91E-03	4.46E-02
hM-enriched (hF vs hM)								
GOTERM_BP_DIRECT	cilium movement involved in cell motility	0.0	11	314	21	12796	1.85E-11	1.63E-08
GOTERM_BP_DIRECT	flagellated sperm motility	0.0	12	314	31	12796	8.62E-11	3.81E-08
GOTERM_BP_DIRECT	cilium movement	0.0	8	314	26	12796	2.16E-06	3.18E-04
GOTERM_CC_DIRECT	9+2 motile cilium	0.0	8	334	11	13739	1.40E-09	1.55E-07
GOTERM_CC_DIRECT	dynein complex	0.0	11	334	32	13739	2.46E-09	1.81E-07
GOTERM_CC_DIRECT	sperm flagellum	0.0	10	334	34	13739	7.97E-08	2.93E-06
GOTERM_CC_DIRECT	motile cilium	0.0	9	334	46	13739	1.28E-05	3.53E-04
GOTERM_CC_DIRECT	cilium	0.0	11	334	86	13739	4.23E-05	1.04E-03
GOTERM_CC_DIRECT	ciliary basal body	0.0	8	334	66	13739	1.05E-03	1.46E-02
GOTERM_CC_DIRECT	outer dynein arm	0.0	5	334	10	13739	6.34E-05	1.40E-03
GOTERM_CC_DIRECT	inner dynein arm	0.0	4	334	8	13739	7.22E-04	1.14E-02
GOTERM_MF_DIRECT	dynein light intermediate chain binding	0.0	10	316	20	12822	3.85E-10	1.46E-07
GOTERM_MF_DIRECT	dynein intermediate chain binding	0.0	11	316	35	12822	7.40E-09	9.34E-07
KEGG_PATHWAY	Motor proteins	0.1	20	110	116	3736	4.02E-10	3.02E-08
dM-enriched (dM vs hM)								
GOTERM_CC_DIRECT	extracellular region	0.2	16	87	765	13739	7.17E-05	6.02E-03
hM-enriched (dM vs hM)								
GOTERM_BP_DIRECT	flagellated sperm motility	0.0	15	285	31	12796	9.44E-16	7.57E-13
GOTERM_BP_DIRECT	cilium movement involved in cell motility	0.0	13	285	21	12796	2.75E-15	1.10E-12
GOTERM_BP_DIRECT	cilium movement	0.0	9	285	26	12796	5.89E-08	7.88E-06
GOTERM_BP_DIRECT	cilium assembly	0.0	12	285	88	12796	3.73E-06	4.27E-04
GOTERM_BP_DIRECT	inner dynein arm assembly	0.0	5	285	10	12796	4.49E-05	4.50E-03
GOTERM_BP_DIRECT	outer dynein arm assembly	0.0	5	285	13	12796	1.45E-04	1.06E-02
GOTERM_CC_DIRECT	9+2 motile cilium	0.0	10	302	11	13739	5.47E-14	5.68E-12
GOTERM_CC_DIRECT	dynein complex	0.0	14	302	32	13739	4.95E-14	5.68E-12
GOTERM_CC_DIRECT	cilium	0.1	17	302	86	13739	4.60E-11	2.39E-09
GOTERM_CC_DIRECT	sperm flagellum	0.0	12	302	34	13739	8.50E-11	3.54E-09
GOTERM_CC_DIRECT	inner dynein arm	0.0	6	302	8	13739	2.59E-07	7.70E-06
GOTERM_CC_DIRECT	motile cilium	0.0	9	302	46	13739	6.12E-06	1.41E-04
GOTERM_CC_DIRECT	outer dynein arm	0.0	5	302	10	13739	4.27E-05	7.41E-04
GOTERM_CC_DIRECT	ciliary basal body	0.0	9	302	66	13739	9.22E-05	1.47E-03
GOTERM_MF_DIRECT	dynein light intermediate chain binding	0.0	12	286	20	12822	7.59E-14	2.45E-11
GOTERM_MF_DIRECT	dynein intermediate chain binding	0.0	13	286	35	12822	6.11E-12	9.84E-10
KEGG_PATHWAY	Motor proteins	0.1	22	91	116	3736	1.01E-13	6.98E-12